Cisplatin Interaction with Cysteine and Methionine in Aqueous Solution: Computational DFT/PCM Study

Tomáš Zimmermann,[†] Zdeněk Chval,[‡] and Jaroslav V. Burda*,[†]

Department of Chemical Physics and Optics, Faculty of Mathematics and Physics, Charles University, Ke Karlovu 3, 121 16 Prague 2, Czech Republic, and Department of Biophysics, Faculty of Health and Social Studies, University of South Bohemia, J. Boreckeho 27, 370 11 Ceske Budejovice, Czech Republic

Received: August 27, 2008; Revised Manuscript Received: December 2, 2008

In this paper we explore cisplatin interactions with sulfur-containing amino acids in a polarizable continuum model. Two cisplatin hydrated complexes were considered as reactants (chloro complex, *cis*-$[Pt(NH_3)_2Cl(H_2O)]^+$; hydroxo complex, *cis*-$[Pt(NH_3)_2(OH)(H_2O)]^+$). We considered the following reaction mechanism: first step, substitution of the aqua ligand by amino acid; second step, dissociative chelate formation. For the optimized complex (at the B3LYP/6-31+G(d)/COSMO level), the energy profile was determined using the B3LYP/6-311++G(2df,2pd) level and two different PCM models—COSMO and UAKS/DPCM methods which were adapted for use on transition metal complexes. The results show thermodynamic preference for bonding by cysteine sulfur followed by the amino group nitrogen, methionine thioether sulfur, and carboxyl-group oxygen. Methionine slightly prefers the Pt−N(Met) coordination in the chloro complex, but in the hydroxo complex it prefers the Pt−S(Met) coordination. A similar trend follows from the bonding energies: BE(Pt−S(Cys)) = 80.8 kcal/mol and BE(Pt−N(Met)) = 76 kcal/mol. According to the experimental observations, the most stable structures found are κ^2(S,N) chelates. In the case of methionine, the same thermodynamic stability is predicted also for the κ^2(N,O) chelate. This differs from the gas-phase results, where κ^2(S,N) and even κ^2(S,O) were found to be more stable than κ^2(N,O) complex.

Introduction

Cisplatin (*cis*-diamminedichloroplatinum(II)) is one of the most commonly used anticancer agents. It is administered intravenously, and on its way into the cell it can interact with blood proteins[1] and other macromolecules. Inside the cellular environment with a significantly lower chloride concentration cisplatin undergoes hydrolysis, which leads to the formation of more reactive positively charged aqua complexes. These complexes can further interact with a wide spectrum of biomolecules including RNA, DNA, cellular proteins, peptides, and others.[2] A crucial step in the cisplatin antitumor activity is (most probably) formation of DNA−platinum bifunctional adducts. The most preferred platinum DNA binding sites are the N7 positions of guanine nucleobases. Cisplatin isomer—*trans*-diamminedichloroplatinum(II)—is inactive. This could be attributed to the fact that due to the 180° angle between the leaving groups transplatin forms different adducts with DNA. In particular, unlike cisplatin, it is unable to create a bridge between two adjacent guanine bases.[3,4]

Cisplatin and its hydrated products interact with proteins either by direct interaction[5] or by protein recognition of platinum−DNA adducts.[4,6−11] One of the most frequently studied platinum binding sites of proteins are sulfur atoms of cysteine or methionine residues.[3] In both residues sulfur atom is present in different chemical contexts. In cysteine, sulfur belongs to the terminal thiol group, which is capable of deprotonation. At physiological pH some fraction is due to its pK_a (8.3) present in the anionic deprotonated form. In methionine, sulfur is present as thioether with slightly positive partial charge. As will be shown in this work, this difference is a crucial factor that affects the behavior of both amino acids toward cisplatin.

One of the most abundant molecules containing cysteine is glutathione. Glutathione (GSH) is a cellular tripeptide which is inside the cell present in high (0.1−10 mM) concentrations.[12] It has various functions; most notably it serves as a thiol−disulfide redox buffer of the cell,[13] protects from oxidative stress, participates in detoxification mechanism, and takes part in leukotriene synthesis. The platinum−glutathione complex represents a major cisplatin metabolite which accounts for approximately 60% of the intracellular platinum.[14] Several cisplatin−glutathione structures were reported, including dinuclear Pt_2S_2 complexes or κ^2(S,N) chelates.[15] It was shown that these adducts irreversibly inhibit thioredoxin, glutaredoxin, and thioredoxin reductase enzyme,[16,17] and in this manner worsens the ability of the cell to resist oxidative stress. Moreover, metabolism of the cisplatin−glutathione adduct in proximal tubule cells contributes to a strong cisplatin nephrotoxicity. In the respective metabolic pathway, the cisplatin−glutathione adduct is first cleaved by γ-glutamyl transpeptidase and aminopeptidase to yield cysteine κ(S) monodentate platinum complex, which is further cleaved in the reaction catalyzed by cysteine−*S*-conjugate β-lyase.[18,19] Reactive thiol species which are final products of this pathway bind to the macromolecules, triggering an increase of the free cytosolic calcium and finally the cell death. Interestingly, glutathione adduct of a cisplatin non-nephrotoxic analogue carboplatin is probably not metabolized through this pathway.[19] On the other hand, glutathione is also a vital part of cisplatin detoxification mechanism and ATP-dependent GS−Pt efflux is supposed to contribute to its elimination from the cell.[14] Suppression of GSH synthesis can

* To whom correspondence should be addressed. Phone:+420 221 911 246. Fax: +420 221 911 249. E-mail: burda@karlov.mff.cuni.cz.
[†] Charles University.
[‡] University of South Bohemia.

10.1021/jp807645x CCC: $40.75
Published on Web 02/19/2009

even revert cisplatin resistance.[20,21] Other thiol group containing molecules which in vivo interact with cisplatin are cysteine itself and various proteins. The interaction with cysteine residues of many proteins probably contributes to the cisplatin side effects.[22]

With methionine, cisplatin forms various monodentate and bidentate compounds, mainly *cis*-$[Pt(NH_3)_2Met\text{-}(S,N)]^{1+/2+}$ chelates.[23,24] In strongly acidic conditions (pH < 0.5) initial formation of *cis*-$[Pt(NH_3)_2Met\text{-}(S,O)]^{2+}$ was observed, which was subsequently slowly replaced by a more stable *cis*-$[Pt(NH_3)_2Met\text{-}(S,N)]^{2+}$ complex.[25] $[Pt(Met\text{-}(S,N))_2]$ bischelates were also observed in the urine of patients treated with cisplatin.[26,27] In the competitive experimental studies was shown that platinum and the thioether group of methionine forms a weaker bond than platinum and the thiol and even displacement of κ^2(S,N) chelated methionine from a model platinum complex by GSH was observed.[26] Similar result was obtained in a competition study of thioether glutathione analogue GSMe with 5-GMP. The platinum bond to N7 of 5-GMP was found to be more stable than the platinum−thioether bond in Pt(dien)−GSMe, and prior formation of Pt−S bonds even accelerated the Pt−GMP coordination.[28] Nevertheless, in reaction with macromolecular DNA oligomers, the methionine presence inhibits Pt−DNA binding.[29] The interaction with methionine-containing peptides can, similarly to the cysteine case, lead to a disruption of their function, and even hydrolytic cleavage of methione-containing peptides mediated by cisplatin was reported in recent works.[30,31] During a reaction with both cysteine and methionine, the release of ammonia was observed, which is faster for cysteine.[15,23,25,32] Strong sulfur trans effect and trans influence can contribute to the ammonia release,[33,34] and this mechanism can possibly lead to cisplatin inactivation.[33]

The kinetics of cisplatin bonding to S-donor atoms of glutathione, cysteine, and methionine is experimentally relatively well-documented,[32,35−39] and computational study on this theme was published recently.[40] On the other hand, knowledge of equilibrium thermodynamics of these interactions is mediated mainly through the competitive studies performed on model systems. In this work we used the methods of computational chemistry to obtain information about thermodynamics of bonding of cisplatin aquation products to free cysteine and methionine, which can be hardly accessible by other methods.

Many other computational works were devoted to the study of the Pt(II) interaction in bioenvironment. A recent work studying the influence of GC base pairing on the Pt complexes was published,[41] where the possibility of the interbase proton transfer from G to C is discussed. The structural and spectroscopic data for novel platinum-based anticancer drugs are discussed by Dal Peraro[42] using Carr-Parinello molecular dynamics (CPMD) and hybrid molecular mechanics/CPMD techniques. The calculation of the Pt(II) adduct with thiazole was performed by Chang.[43] Dos Santos et al.[44] have studied the structure and properties of a anhydrotetracycline−platinum(II) complex. These authors also dealt with the description of cisplatin in explicit water solution using the Monte Carlo method[45] and the interaction of cisplatin with guanine.[46] Robertazzi et al. have carried out the QM/MM calculations of the cisplatin adduct with an octamer of double-stranded DNA sequence.[47−49] Wysokinski has investigated characterization of the structural and vibrational spectra of (orotato)platinum(II) complex.[50] He has compared the calculated (DFT/mPW1PW91) vibration transitions with experimental data. Some novel trans-platinum(II) anticancer drugs (with aliphatic amines) were studied at the B3LYP level,[51] where also the aquation process was examined. Recently also dinuclear[52] and trinuclear[53] (BBR3464) platinum(II) complexes were studied using the computational approach. Aquation study of carboplatin was performed by Pavelka,[54] where a relatively high activation barrier of 30 kcal/mol was suggested on the basis of the B3LYP/6-31++G(2df,2pd) computational level. Discussion about correlation between thermodynamic and kinetic data and theoretical calculations of the Pt(II) complexes was published by Hofmann et al.[55] A lot of studies on behavior and properties of the platinum complexes were published by Ziegler and co-workers.[56] In one of these studies the activation of methane by $[PtCl_4]^{2-}$ was examined in the acidic aqueous solution. The authors have shown that the complex with two water molecules is the most active in the H/D exchange reaction.[57] Some aspects of the cisplatin hydrolysis are discussed by Tsipis.[58] Some other recent studies on the interaction of Pt(II) complexes should be also mentioned.[25,59−63]

In this work we focus our attention on the interaction of hydrated cisplatin with the sulfur-containing amino acids methionine and cysteine since both are important in vivo cisplatin targets. Taking into account the HSAB principle,[64] a strong platinum affinity to the sulfur sites could be expected.

Computational Details

In our previous work we have explored the cisplatin interactions with sulfur-containing amino acids in the gas-phase model.[34] We chose the DFT/B3LYP computational level and compared it with several other methods (including the CCSD(T)) on model system *cis*-$[Pt(NH_3)_2(H_2S)(OH)]^+$). In the present work we use the DFT/B3LYP method for both geometry optimizations and single-point calculations. Combination of the B3LYP functional method with the COSMO solvation model was successfully used in the study comparing the relative stability of cis and trans cisplatin isomers.[65] On the other hand, in the study,[66] where several computational methods were compared with experimental geometric parameters and vibrational frequencies of cisplatin and carboplatin, the mPW1PW functional was suggested as the best computational tool for these systems. However, the differences in calculated geometric parameters between the B3LYP and mPW1PW functionals were small. Moreover in our previous study, the B3LYP functional reproduced the CCSD(T) bonding energy of the Pt−S bond significantly better than mPW1PW.

The Stuttgart-Dresden quasi-relativistic energy-averaged pseudopotentials were used to describe core electrons of platinum (MWB-60[67]), chlorine, and sulfur (MWB-10[68]). The 6-31+G* basis set was chosen, and the original pseudoorbitals of Pt, Cl, and S atoms were augmented by appropriate diffuse and polarization functions ($\alpha_f(Pt) = 0.980$, $\alpha_d(Cl) = 0.618$, and $\alpha_d(S) = 0.498$).[69] For the single-point (SP) calculations the triple-ζ 6-311++G(2df,2pd) basis set was used with pseudoorbitals of heavy elements augmented by the same diffuse functions and the following set of polarization functions: $\alpha_{f1}(Pt) = 1.419$, $\alpha_{f2}(Pt) = 0.466$, $\alpha_g(Pt) = 1.208$; $\alpha_{d1}(Cl) = 1.500$, $\alpha_{d2}(Cl) = 0.375$, $\alpha_f(Cl) = 0.700$; $\alpha_{d1}(S) = 0.918$, $\alpha_{d2}(S) = 0.289$, and $\alpha_f(S) = 0.568$.[69]

To include the effects of water as a high-permittivity solvent, we utilized the SCRF computational framework. Geometry optimizations were performed using the COSMO method with sphere radii proposed by Klamt.[70] In SP calculations two implicit solvation models were applied: (a) the COSMO method as specified above and (b) the DPCM model[71,72] with modified UAKS cavities.[73] In the latter case, the polarization charges were compensated by means of an additional effective charge distributed according to the solute electronic density (ICOMP

= 4 keyword in Gaussian 03 program). It should be mentioned that the study[73] introduces the UAHF model optimized for the HF/6-31G* level of theory and not the UAKS model, which is optimized for the PBE0/6-31G(d) level. But the only difference between both (in our case) consists of the sphere radii of sp_2 hybridized oxygen. Since UAKS cavities were not optimized for the transition metal complexes, small modifications were necessary to appropriately describe solvation of platinum complexes. Sphere radii in ref 73 were calculated considering the atom type, number of bonded hydrogens, hybridization, atomic charge and effects of neighboring groups. The originally used atomic charge is a formal charge carried by atoms in ions or zwitterions (for example oxygens of the deprotonated carboxyl group both possess formal charge $-1/2$). For groups of platinum complexes this model due to the lack of the parametrization assigns charges which are equal to the total charge of the complex divided by the number of groups. Instead we attempted to assign formal partial charges of platinum ligands in a manner similar to UAKS of organic molecules. This approximation appeared to be too crude. Therefore, more realistic NPA partial charges from the COSMO single-point calculations were applied instead of the formal charges. However, NPA partial charges cannot be used directly in the UAKS model since it is parametrized using formal charges (the original atomic radii, beside other criteria, reflects the (semi-)integer charge localized on the atom, e.g., for sulfur: $R_S = 1.980 + fn$, where n is the formal charge and f is some fitted factor ($f(S) = 0.3$)). Therefore we have introduced a scaling procedure for NPA partial charges of platinum ligands (containing sulfur, chlorine, nitrogen, and oxygen) based on the actual NPA charges of reference molecules, which were used or were similar to molecules used for parameterization of the original model. [For instance, sulfur atom bonded to platinum has a charge from the range between the neutral CH_3SH ($n = 0$) and the anion CH_3S^- ($n = -1$) states. In the scaling procedure, the NPA charge of S atom from the Pt complex (with cysteine or methionine) was determined first, then projected into the range of NPA charges of sulfur in CH_3SH and CH_3S^- particles, and linearly rescaled into the $-1 - 0$ range of formal charges. This procedure gives a better estimation for n in R_S parametrization when compared to the original article.[73]] The performance of this modification of the UAKS model was verified by means of comparison with experimental pK_a values of the *cis*-$[Pt(NH_3)_2(H_2O)_2]^{2+}$, *cis*-$[Pt(NH_3)_2(OH)(H_2O)]^+$, and *cis*-$[Pt(NH_3)_2Cl(H_2O)]^+$ complexes. The details of the procedure together with the comparison with other methods and experimental values can be found in the article.[74] Superior performance of the original DPCM/UAHF method in this type of calculation was also observed by da Silva et al.[75] in calculations of pK_a of nitrous acid.

Calculating the thermochemical data, we have found that although all the structures were properly optimized using standard convergence criteria, some vibrational spectra (even after subsequent optimization attempts) still contained very low imaginary frequencies. This is the most probably due to the numerical instability of PCM method caused by a discretization of a cavity surface. Therefore in determination of the Gibbs free energies, the vibrational analyses were taken from gas-phase (reoptimized) calculations at the HF/6-31+G* level of theory. The average gas phase − solvent difference of thermal corrections to the Gibbs free energy determined for all molecules, where the solvent vibrational spectrum without imaginary frequencies was obtained, is 9.4 kcal/mol (thermal corrections to Gibbs free energy taken from solvated molecules are always lower). This averaged difference correlates well with the number of degrees of freedom of a particular molecule with an average value of 0.14 kcal/mol per degree of freedom (neglecting error in rotational frequencies) and variance of 0.017 kcal/mol (average absolute deviation is only 10% of the mean). Thus, the probable error introduced to the reaction Gibbs free energies by using the HF gas-phase frequencies instead of the COSMO frequencies is approximately 1.5 kcal/mol (deviations in reactants and products are taken as mutually uncorrelated). The true COSMO frequencies were used in two cases (where no imaginary eigenvalues occurred): First, in a detailed discussion of solvent influence on properties of both *cis*-$[Pt(NH_3)_2Cl(H_2O)]^+$ and *cis*-$[Pt(NH_3)_2(H_2O)(OH)]^+$ reactant complexes. Second, in the discussion of the relative stability of κ^2(S,N) methionine chelates, where higher accuracy is needed in comparison of subtle energy differences of various nearly degenerated conformers, which were observed in the NMR measurements.

Another source of error arises from the fact that in a solvent a mixture of several geometric conformers of a same complex is usually present. The ratio of their concentrations is determined by the Maxwell−Boltzmann statistics. In our calculations, only global minima are, however, used. This error affects more results obtained within supermolecular approach, because of the higher number of conformations available for weakly bound supermolecules. Structures of global minima were obtained from several (usually above 10) local minima examined at the B3LYP/6-31+G* level. Usually, for both reactant and product four to five other structures were within 2−3 kcal/mol from a global minimum. Therefore, large cancelation of errors can be expected on the basis of this similarity. To estimate the error numerically, we consider a reaction where reactant can take only one conformation, whereas product can take either one conformation or 10 degenerated but distinguishable conformations. Standard reaction Gibbs free energy in the first case is equal to

$$\Delta G_1 = -RT\ln(K_1) = -RT\ln\left(\frac{Q_p}{Q_r}\right) \quad (1)$$

where Q_r and Q_p are partition functions of reactant and of the product. In the second case 10 times more states are accessible to the product, so the standard reaction free energy is

$$\Delta G_2 = -RT\ln(K_2) = -RT\ln\left(\frac{10Q_p}{Q_r}\right) = \Delta G_1 - RT\ln(10) \quad (2)$$

The error caused by neglecting nine conformers of product at 298.15 K is therefore equal to 1.36 kcal/mol. If that nine conformers had higher formation Gibbs free energies than the global minimum, their contribution to the partition function would be exponentially suppressed and the error greatly reduced. For example if all nine conformers had 1 kcal/mol higher formation Gibbs free energy, then the error caused by neglecting them would be only 0.35 kcal/mol. From this and aforementioned large cancelation of errors between reactant and products, it can be expected that the error caused by neglecting all local minima is safely well beyond 0.5 kcal/mol.

Three energy characteristics were calculated in the COSMO approach to investigate a weak association of the monomers in supermolecules: (a) association energy without the deformation energy

$$\Delta E_S^{af} = E_{supermol}^{el} + G_{supermol}^{sol} - \sum_{m}^{monomers} (E_m^{el} + G_m^{sol}) \quad (3)$$

where G^{sol} represents electrostatic, cavitation, dispersion, and repulsion solvation free energy terms calculated in the SCRF framework. Monomer energies are calculated in the frozen supermolecular geometry. Subscript S denotes that both supermolecule and monomers were surrounded by the solvent. Adding the G^{sol} terms to E^{el} actually creates a mixed quantity, which does not have a direct thermodynamic sense (it is neither the Gibbs free energy nor energy since it does contain part of the work necessary to introduce the molecule into the dielectric). But it is useful in this context, and in our model it also has a convenient property of temperature independence.

(b) association energy with deformation corrections

$$\Delta E_S^{a} = \Delta E_S^{af} + \sum_{m}^{monomers} \Delta E_m^{deform} \quad (4)$$

(c) association Gibbs free energy (ΔG_S^a) by adding thermodynamic quantities of nuclear motion to association energy.

The bonding energies (BE) of the Pt−L bonds (calculated for isolated Pt complexes) are determined according to eq 3 where instead of monomers two fragments partitioned according to the corresponding Pt−L bond were regarded.

To correct for the basis set superposition error,[76,77] the electronic energies of separated molecules were calculated using a complete set of basis functions of all atoms present in the supermolecule. Two counterpoise-like procedures were employed. In the first one, energies of fragments enclosed in appropriate cavities were calculated in the basis set of a complete supermolecule with the ghost atoms placed mainly outside the fragment cavity. Unfortunately this leads to the incorrect values of solute−solvent energies of nonelectrostatic origin (at least in our version of Gaussian03 Rev.C2). Nevertheless these energies can be taken from calculations of, e.g., the deformation energy corrections where an isolated monomer without ghost atoms must be employed. In the second approach to the BSSE corrections, a sum of differences of monomer electronic energies computed in the basis set of the supermolecule (with ghost atoms) and in the basis set of the monomer (without ghost atoms) was determined where both energies were calculated in the cavity of the supermolecule. This BSSE correction was added to the association energy computed as a simple difference of electronic energy of a supermolecule and sum of electronic energies of monomers without ghost atoms. Both methods are illustrated in Figure 1.

The average absolute BSSE correction in the whole set of calculated complexes is 0.93 kcal/mol (using the first method), and the average absolute difference between both methods is 0.09 kcal/mol. The largest difference between both BSSE approaches is 0.5 kcal/mol in the case of strongly bonded Pt(II) and −1 charged cysteine, where the bonding energy is 127.6 kcal/mol and the BSSE correction using the first method is 1.6 kcal/mol. The estimation of BSSE corrections using the first approach is used in further discussion.

Partial charges analysis was done using the natural bond orbitals program NBO v. 5.0[78] at the B3LYP/6-311++G(2df,2pd) level of theory in the COSMO solvation model.

Results and Discussion

The two most important cisplatin hydrolysis products *cis*-$[Pt(NH_3)_2Cl(H_2O)]^+$ and *cis*-$[Pt(NH_3)_2(OH)(H_2O)]^+$ were chosen as mono- and dihydrated reactants. The studied reaction mechanism leading to formation of chelate product through a monodentate intermediate was studied in the model of isolated molecules and in the supermolecular model where reactants and products form the associated complex. In the first reaction step (the least firmly) bound aqua ligand of the hydrated cisplatin cation is replaced by the amino acid. Preference of the aqua ligand is also suggested by results of numerous experimental studies, e.g., in refs 32 and 79. All three possible active sites (S, N, and O atoms) of the amino acid were considered for the formation of dative bonds with the platinum atom. In the second step, one of the two remaining free active sites of the amino acid further replaces the second Pt−ligand (either chloride or hydroxyl group) forming the chelate structure. Other possible reaction paths (e.g., replacement of the NH_3 ligands) were not considered, although these species were also observed in the reaction of methionine with nonhydrated cisplatin[23] with more labile leaving ligands such as aqua in *cis*-$[Pt(NH_3)_2(H_2O)_2]^{2+}$. Nevertheless, these structures were not observed in significant quantities.[15] Since the reactions take place in an aqueous solution, a rapid establishment of equilibrium with respect to the proton-transfer reactions is assumed. All possible internal proton transfers were taken into account. Generalization of this approach to the case where protons are exchanged also with solvent will be the subject of our subsequent study.

Structures. Structures of the most stable conformers discussed in the study are presented in Figures 2−4. In contrast to the gas-phase calculations, solvation introduces several structural changes. When solvated, amino acids adopt zwitterionic structure. The calculated cysteine structure can be compared to the global minimum found in the computational study devoted to the solvation of cysteine.[80] The accordance is qualitative and the main reason of the quantitative disagreement can be seen in fact that, in the Fernandez-Ramos' study,[80] the Onsager solvation model was used for geometry optimization. In the platinum chloro complex, solvation leads to weakening of the Pt−Cl bond accompanied by bond elongation by approximately 0.06 Å and a 40 cm^{-1} red shift of the bond stretch frequency to 309 cm^{-1}. Also, the NPA negative charge of chlorine increases by 0.14 e. Other coordination distances are consequently shortened, most notably the platinum−ammine ligand in the trans position to Cl^- anion is shortened by 0.06 Å. Its stretch frequency is shifted up by approximately 50 cm^{-1} due to the weakening of chlorine trans influence. Also the Pt−O bond in the hydroxo complex is lengthened by approximately 0.04 Å accompanied with a bond stretch frequency shift down by 50 cm^{-1} to 548 cm^{-1}. The NPA negative charge of the oxygen atom is increased by approximately 0.05 e. In analogy with the chloro complex the trans Pt−NH_3 bond is shortened by approximately 0.04 Å with the frequency shifted up by approximately 40 cm^{-1}.

Although charged systems do not have an invariant dipole moment under translation, keeping the origin of the coordinate system in the center of the mass of structures, some interesting features can be shown. In both complexes, the changes related to the solvation lead to an increase of the molecular dipole moment by approximately a half—to 11.1 (chloro complex) and 8.9 D (hydroxo complex). As for amino acids; an increase of the dipole moment is further enhanced by adoption of the zwitterionic structure; the solution values are 2.5 (cysteine) and 3 (methionine) times higher than the gas-phase ones. This trend is conserved in all first- and second-step products, and the average dipole moment of solvated molecules is approximately 2.5 times larger than in the gas phase.

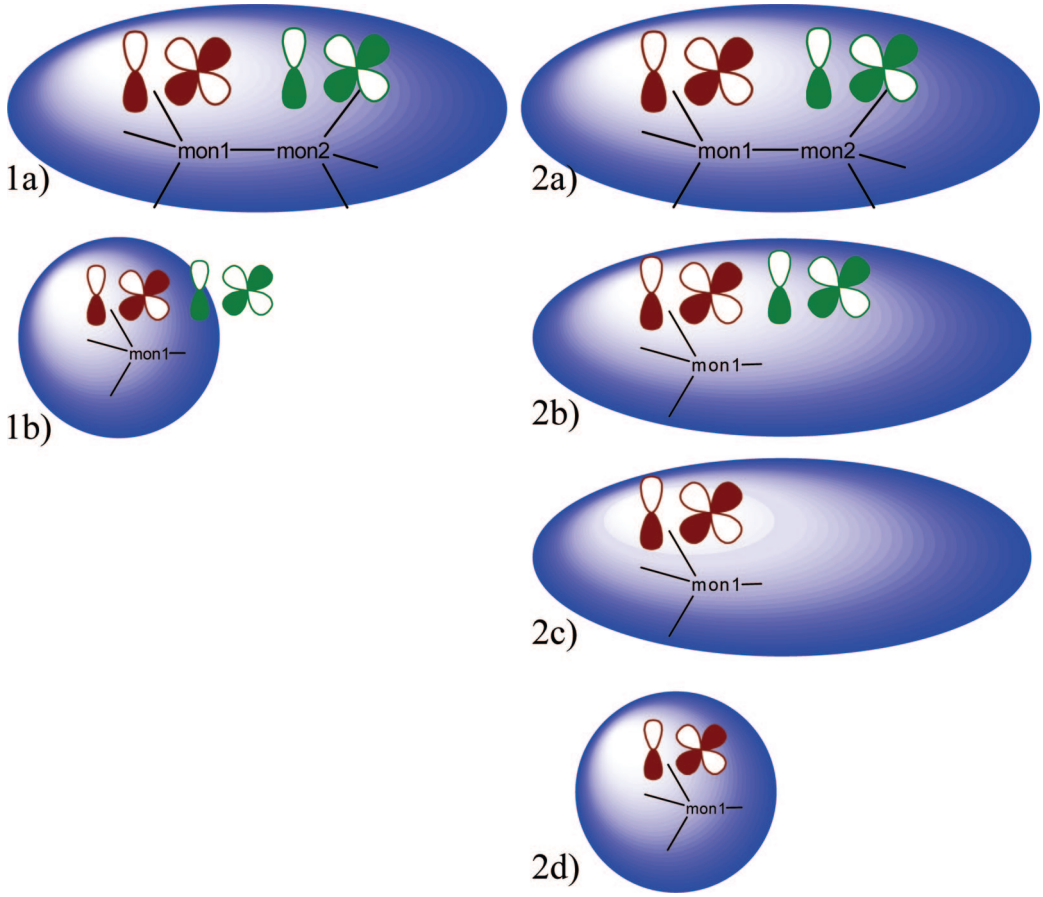

Figure 1. Counterpoise-like BSSE calculations. In the first method, ΔE_S^{af} is calculated as a difference between the energy of supermolecule 1a and a sum of fragment energies calculated in supermolecular basis set using fragment cavities 1b. In the second approach, $\Delta E_S^{af} - E^{BSSE}$ is calculated as a difference between the energy of supermolecule 2a and a sum of fragment energies calculated in the fragment basis set using fragment cavities 2d. E^{BSSE} is calculated as a sum of differences of fragment energies calculated in supermolecular 2b and fragment 2c basis sets both in the supermolecular cavity.

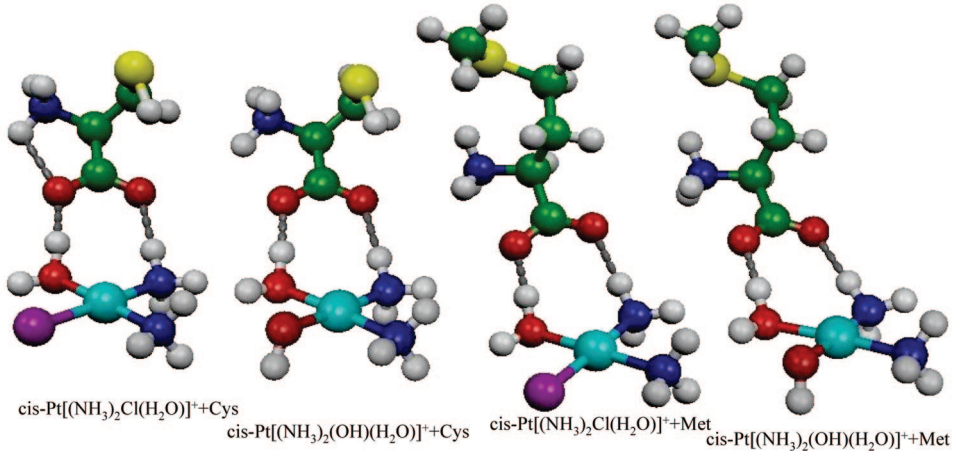

Figure 2. First-step reactants in the supermolecular approach.

In the products of the first reaction step, the aqua ligand is substituted by the amino acid donor atom. The most stable supermolecular structures are displayed in Figure 2. The coordination distances of the platinum atom are presented in Table 1. Partial charges of platinum and its ligands are summarized in Table 2.

The sulfur coordination is accompanied by a charge transfer from the sulfur to platinum atom whose partial charge is decreased by approximately 0.17 e. This value is similar for both cysteine and methionine, suggesting that the extent of electron donation is comparable for both amino acids. The main difference between the thiol and thioether dative bonds lies in the different ionic character of both bonds. Whereas the positive partial charge of methionine sulfur is increased during the bond formation by 0.28 to 0.48 e, the partial charge of cysteine sulfur is decreased by +0.25 to −0.28 e due to additional proton transfer from very acidic platinum-bonded sulfur to carboxyl oxygen. This way, the Pt−S bond in cysteine complexes gains significantly more ionic character. This fact can be demonstrated also on the example of two point charges (using the NBO charges of platinum and sulfur atoms of cysteine or methionine) in the optimized bond distances. The gas-phase difference of

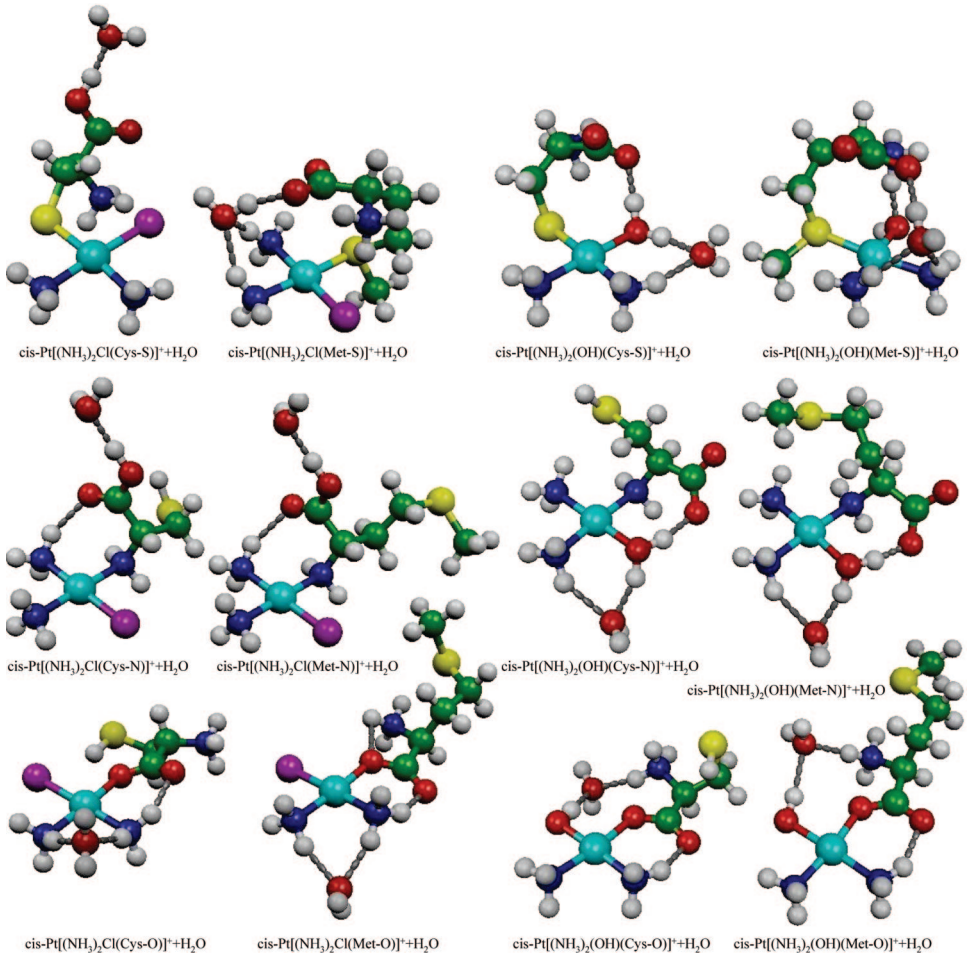

Figure 3. First-step products in the supermolecular approach.

electrostatic energies of point charges representing cysteine and methionine complexes is approximately 50 kcal/mol, which is very similar to the difference of the gas-phase bonding energies calculated in our previous paper.[34] The Pt−S bond length of 2.35 Å is unaffected by the solvent and is practically independent of the complex type. A similar insensitivity of the Pt−S bond length on the type of the sulfur ligand can also be observed in the results of the study,[81] where the *cis*-$[Pt(NH_3)_3L]^{2+}$ complexes were explored (L is a small ligand containing either S, N, or O donor atoms). The Pt−S bond length obtained for all the complexes calculated in ref 81 was 2.32 Å, and the same value is also an average of the Pt−S distances found in the X-ray diffraction study of +2 charged platinum complex $[Pt(tu)_4]Cl_2$ (tu = thiourea).[82] All these data give a fair confidence in our results. Previously mentioned internal proton transfer from platinum-bonded sulfur to carboxylic oxygen occurs only in chloro complexes, since in the hydroxo complex *cis*-$[Pt(NH_3)_2(OH)(Cys\text{-}S)]^+$, the higher acidity of cysteine carboxylic group leads to a proton transfer to the platinum hydroxo ligand instead, so that the most stable structure is actually *cis*-$[Pt(NH_3)_2(H_2O)(Cys\text{-}S)]^+$. This effect was not observed in the gas-phase calculations.

Nitrogen coordination causes only a slight decrease of the platinum charge by approximately 0.04 e (in comparison to the original reactant complexes), demonstrating a lower donation of the amino group compared to sulfur. The Pt−N bond length is approximately 2.1 Å, which is also the gas-phase value. The structures of chloro complexes (with both amino acids) are stabilized by internal hydrogen bonds between the platinum ammine ligand and the carboxyl group of amino acid. The hydroxo complexes undergo an internal proton transfer from the carboxyl groups, transforming the hydroxo ligands into aqua ligands. The aqua ligand remains H-bonded to the carboxyl group (cf. Figure 3).

Coordination of oxygen does not affect the platinum partial charge. The Pt−O bond distance is 2.07 Å, which is approximately by 0.03 Å longer than in the corresponding gas-phase structures. In the chloro complexes, one of the ammine ligand forms a hydrogen bond with the carboxyl group, which is tilted by approximately 35° out of the platinum complex plane. In the hydroxo complexes a stronger hydrogen bond is formed between the hydroxo ligand and carboxyl group in the plane of the platinum complex.

In the second reaction step, the remaining leaving ligand (either chloride or (possibly protonated) hydroxide) is replaced by the second amino acid donor atom and the chelate structure is formed. The Pt−X distances (where X is a donor atom of amino acid) are usually shortened in comparison to monodentate complexes. This is most significant in the case of +1 e charged κ^2(N,O) complexes where both Pt−N and Pt−O bonds are by 0.04 Å shorter than in the corresponding monodentate complexes. All the κ^2(N,O) structures contain a rigid five-membered ring with the plane of the carboxyl group practically coplanar with the plane of the platinum ligands. The carboxyl group is protonated in the +2 complexes and deprotonated in the +1 e charged complexes (cf. structures in the middle part of Figure 4).

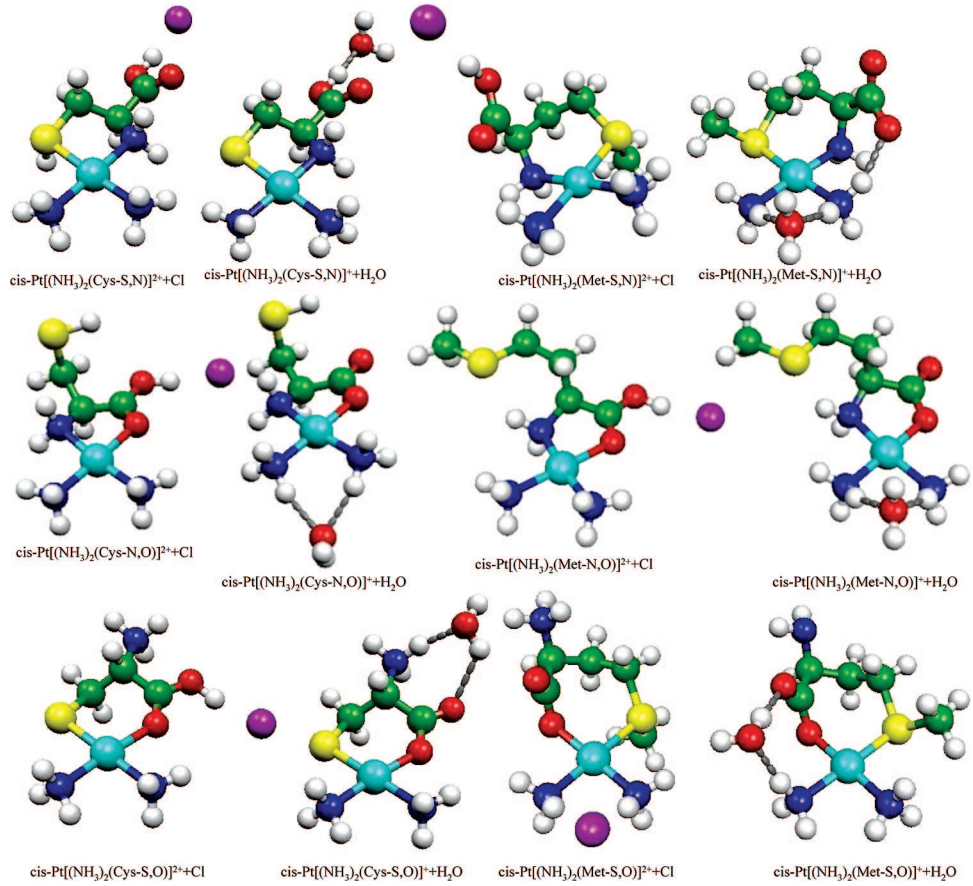

Figure 4. Second-step products in the supermolecular approach.

Regarding the κ^2(S,N) chelates, each amino acid adopts a different conformation. Since cysteine has a shorter side chain, the five-membered ring with the carboxyl group in equatorial position is formed in accord with the structure proposed for *S*-methyl-L-cysteine in the study of Appleton et al.[25] The most stable methionine (+2) κ^2(S,N) chelate is a six-membered ring in a chairlike conformation with both carboxy and *S*-methyl groups in axial positions. Slightly twisted boatlike conformation has approximately 1.3 kcal/mol higher energy. In the case of +1 charged chelates (the charge also depends on the pH of the surrounding solvent), practically the same energy was obtained for both conformers. The boatlike conformation is very slightly preferred (the difference is less than 0.2 kcal/mol) due to a stronger H-bond between the deprotonated carboxyl group and the platinum ammine ligand (in boatlike conformation H-bond is shorter and, also, the N···H−O bond is closer to 180°). This constrasts to the structure found in the X-ray diffraction study of *cis*-[Pt(Cl)$_2$(Met-S,N)],[83] where the chairlike conformation with equatorial carboxyl and *S*-methyl groups was observed. Subsequently in the NMR experimental study of cisplatin methionine chelate,[15] the equatorial position of the carboxyl group is assumed. However, our calculations show that interaction with the ammine ligand stabilizes the carboxyl group in axial position. Similarly, the *S*-methyl group is stabilized in the axial position by interaction of the sulfur lone pair with hydrogen of the second ammine ligand. A difference in the Gibbs free energies between both S-methyl positions (corresponding to the S and R sulfur atom chiralities) is relatively small—approximately 0.5 kcal/mol for +1 chelate and 0.4 kcal/mol for +2 chelate (using the more accurate COSMO vibrational frequencies). At room temperature these differences represent a concentration ratio of 2.7:1 and 2:1, respectively. In the mentioned NMR

TABLE 1: Platinum Coordination Distances (Å)[a]

complex[b]	Pt−S	Pt−N(AA)	Pt−O	Pt-X	Pt-Nt	Pt-Nc
[Pt−a$_2$Cl(H$_2$O)]$^+$			2.11	2.36	2.03	2.07
[Pt−a$_2$(OH)(H$_2$O)]$^+$			2.10	2.01	2.03	2.09
[Pt−a$_2$Cl(Cys-S)]$^+$	2.35			2.38	2.12	2.07
[Pt−a$_2$Cl(Met-S)]$^+$	2.35			2.37	2.09	2.07
[Pt−a$_2$(OH)(Cys-S)]$^+$	2.35			2.10	2.12	2.04
[Pt−a$_2$(OH)(Met-S)]$^+$	2.34			2.03	2.08	2.08
[Pt−a$_2$Cl(Cys-N)]$^+$		2.09		2.36	2.07	2.07
[Pt−a$_2$Cl(Met-N)]$^+$		2.09		2.36	2.07	2.07
[Pt−a$_2$(OH)(Cys-N)]$^+$		2.10		2.08	2.07	2.05
[Pt−a$_2$(OH)(Met-N)]$^+$		2.10		2.07	2.07	2.05
[Pt−a$_2$Cl(Cys-O)]$^+$			2.07	2.37	2.05	2.07
[Pt−a$_2$Cl(Met-O)]$^+$			2.07	2.37	2.05	2.07
[Pt−a$_2$(OH)(Cys-O)]$^+$			2.07	2.01	2.04	2.09
[Pt−a$_2$(OH)(Met-O)]$^+$			2.07	2.01	2.04	2.09
[Pt−a$_2$(Cys-S,N)]$^{2+}$	2.33	2.08			2.09	2.07
[Pt−a$_2$(Cys-S,N)]$^+$	2.32	2.08			2.13	2.08
[Pt−a$_2$(Met-S,N)]$^{2+}$	2.34	2.08			2.09	2.08
[Pt−a$_2$(Met-S,N)]$^+$	2.35	2.08			2.09	2.09
[Pt−a$_2$(Cys-S,O)]$^{2+}$	2.33		2.08		2.12	2.04
[Pt−a$_2$(Cys-S,O)]$^+$	2.33		2.05		2.12	2.06
[Pt−a$_2$(Met-S,O)]$^{2+}$	2.35		2.05		2.08	2.06
[Pt−a$_2$(Met-S,O)]$^+$	2.36		2.04		2.08	2.07
[Pt−a$_2$(Cys-N,O)]$^{2+}$		2.08	2.07		2.07	2.04
[Pt−a$_2$(Cys-N,O)]$^+$		2.06	2.03		2.07	2.07
[Pt−a$_2$(Met-N,O)]$^{2+}$		2.08	2.07		2.07	2.04
[Pt−a$_2$(Met-N,O)]$^+$		2.06	2.03		2.07	2.07

[a] AA means amino acid; X stands for either Cl or O (of hydroxo ligand); Nt refers to the ammine ligand in the trans position to the aqua ligand in reactant complexes, to the amino acid in the first-step products, to the sulfur atom in κ^2(S,N) and κ^2(S,O) chelate complexes, and to the nitrogen atom in κ^2(N,O) chelates; Nc refers to the remaining ammine ligand. [b] In all chemical formulas, a$_2$ means (NH$_3$)$_2$.

TABLE 2: NPA Partial Charges (e) from the COSMO Approach[a]

complex[c]	Pt	S	X	N^t	N^c	N^a	O^n	O^x
$[Pt-a_2Cl(H_2O)]^+$	0.67		−0.59	−0.89	−0.94			
$[Pt-a_2(OH)(H_2O)]^+$	0.75		−1.08	−0.90	−0.95			
cysteine		−0.03				−0.69	−0.80	−0.82
methionine		0.20				−0.71	−0.81	−0.83
$[Pt-a_2Cl(Cys-S)]^+$	0.49	−0.28	−0.59	−0.97	−0.92	−0.70	−0.65	−0.68
$[Pt-a_2Cl(Met-S)]^+$	0.48	0.49	−0.59	−0.95	−0.94	−0.69	−0.80	−0.81
$[Pt-a_2(OH)(Cys-S)]^+$	0.58	−0.28	−0.90[b]	−0.98	−0.90	−0.68	−0.77	−0.85
$[Pt-a_2(OH)(Met-S)]^+$	0.59	0.47	−1.05	−0.95	−0.94	−0.74	−0.81	−0.82
$[Pt-a_2Cl(Cys-N)]^+$	0.62	−0.01	−0.60	−0.92	−0.94	−0.76	−0.66	−0.68
$[Pt-a_2Cl(Met-N)]^+$	0.62	0.20	−0.60	−0.93	−0.94	−0.75	−0.67	−0.68
$[Pt-a_2(OH)(Cys-N)]^+$	0.72	−0.05	−0.91[b]	−0.93	−0.92	−0.77	−0.77	−0.82
$[Pt-a_2(OH)(Met-N)]^+$	0.72	0.18	−0.91[b]	−0.93	−0.93	−0.77	−0.77	−0.82
$[Pt-a_2Cl(Cys-O)]^+$	0.67	−0.01	−0.61	−0.91	−0.94	−0.68	−0.74	−0.72
$[Pt-a_2Cl(Met-O)]^+$	0.67	0.20	−0.61	−0.91	−0.94	−0.70	−0.74	−0.73
$[Pt-a_2(OH)(Cys-O)]^+$	0.74	−0.02	−1.10	−0.91	−0.95	−0.68	−0.75	−0.73
$[Pt-a_2(OH)(Met-O)]^+$	0.74	0.19	−1.10	−0.91	−0.95	−0.70	−0.75	−0.73
$[Pt-a_2(Cys-S,N)]^{2+}$	0.56	0.30		−0.95	−0.93	−0.76	−0.64	−0.68
$[Pt-a_2(Cys-S,N)]^+$	0.52	−0.25		−0.98	−0.93	−0.76	−0.66	−0.69
$[Pt-a_2(Met-S,N)]^{2+}$	0.54	0.49		−0.96	−0.93	−0.76	−0.66	−0.68
$[Pt-a_2(Met-S,N)]^+$	0.54	0.48		−0.97	−0.94	−0.76	−0.84	−0.81
$[Pt-a_2(Cys-S,O)]^{2+}$	0.59	−0.23		−0.98	−0.89	−0.67	−0.62	−0.64
$[Pt-a_2(Cys-S,O)]^+$	0.57	−0.25		−0.98	−0.91	−0.67	−0.74	−0.74
$[Pt-a_2(Met-S,O)]^{2+}$	0.61	0.48		−0.95	−0.92	−0.67	−0.69	−0.76
$[Pt-a_2(Met-S,O)]^+$	0.60	0.47		−0.95	−0.92	−0.89	−0.71	−0.78
$[Pt-a_2(Cys-N,O)]^{2+}$	0.74	−0.01		−0.93	−0.90	−0.77	−0.62	−0.63
$[Pt-a_2(Cys-N,O)]^+$	0.72	−0.03		−0.94	−0.93	−0.77	−0.71	−0.74
$[Pt-a_2(Met-N,O)]^{2+}$	0.74	0.20		−0.93	−0.90	−0.79	−0.63	−0.63
$[Pt-a_2(Met-N,O)]^+$	0.71	0.19		−0.94	−0.93	−0.78	−0.72	−0.74

[a] X stands for Cl or O (in hydroxo ligand); N^a is the nitrogen of the amino acid, O^n the carbonyl oxygen and O^x the hydroxyl oxygen of the carboxyl group, N^t the nitrogen from the ammine ligand in the trans position to the aqua ligand in reactant complexes, to the amino acid in the first-step products, to the sulfur atom in κ^2(S,N) and κ^2(S,O) chelate complexes, and to the nitrogen atom in κ^2(N,O) chelates; N^c refers to the nitrogen atom from the remaining ammine ligand. [b] Aqua ligand formed by the proton transfer to the hydroxyl group. [c] In all chemical formulas, a_2 means $(NH_3)_2$.

studies two sets of ^{1}H δCH_3 and ^{195}Pt resonances are described and assigned to isomers with different sulfur chiralities with ratios of 5:3[25] and 1.3:1[23] (both measurements were performed in a solution with pH > 5, where +1 charged chelate dominates). Discussed structures are drawn in Figure 5.

Finally in cysteine κ^2(S,O) chelates, planarity of the carboxyl group imposes the six-membered ring flat boatlike structure with the amino group in the equatorial position. Methionine κ^2(S,O) chelate forms a seven-membered ring in a chairlike conformation with the amino and *S*-methyl groups in axial positions.

Reaction Energetics. Reaction energies and reaction Gibbs free energies were calculated using both COSMO and modified DPCM/UAKS solvation models with vibrational frequencies taken from the reoptimized gas-phase structures as discussed in Computational Details. COSMO Gibbs free energies are collected in Table 8 in the Supporting Information; DPCM/UAKS values, in Table 3.

Since the modified DPCM/UAKS model performs much better than COSMO in comparison of calculated and experimental pK_a values, as shown in ref 74, we will concentrate on the DPCM/UAKS results in the discussion of reaction energies. The DPCM/UAKS and COSMO Gibbs free energies usually differ by up to 8 kcal/mol. One exception is the second reaction step in the noninteracting approach (of isolated molecules), where small ions (hydroxide and chlorine) are released. In this case the difference is up to 25 kcal/mol for reactions leading to +2 charged platinum chelates and hydroxide ions (these reactions are always thermodynamically more demanding than the formation of the +1 charged chelate and water molecule; therefore, their Gibbs free energies are not presented hereinafter) and up to 15 kcal/mol for reactions releasing chloride ions. A qualitative difference between both models occurs in the chelation step of cysteine chloro complexes and in the reaction leading to methionine κ^2(N,O) chelate, where formation of +2 chelate is predited in DPCM/UAKS, while +1 chelate and HCl is the most stable product in the COSMO approach. The main source of this discrepancy lies in the difference of solvation

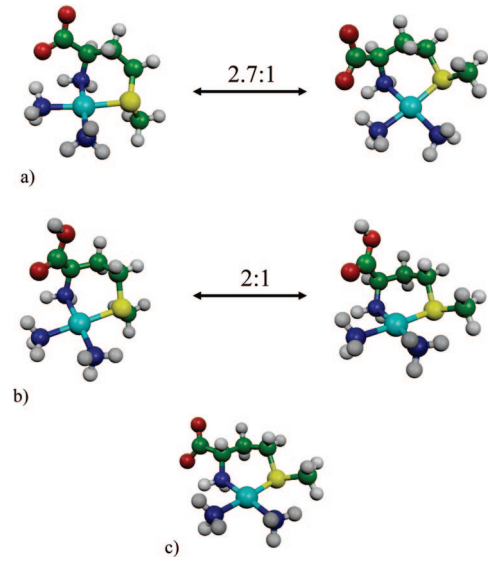

Figure 5. Structures and room temperature concentration ratios of +1 charged (a) and +2 charged (b) *cis*-$[Pt(NH_3)_2(Met\text{-}S,N)]^{1+/2+}$ chelates differing in the position of *S*-methyl groups. Notice the boatlike conformation of the 1+ chelate and the chairlike conformation of the 2+ chelate. In the bottom, the structure originally proposed in ref 25 (c) is depicted.

TABLE 3: Reaction Gibbs Free Energies (kcal/mol) at 298.15 K Using the DPCM Approach with Modified UAKS Cavities

		isolated molecules				supermolecules	
reactants[a]	products[a]	Cys	Met	Cys	Met	Cys	Met
$[Pt-a_2Cl(H_2O)]^+ + AA$	$[Pt-a_2Cl(AA\text{-}S)]^+ + H_2O$	−8.9	1.0	complete reaction energies (energy difference of first step reactants and second step products plus water molecule)		−11.8	5.9
	$[Pt-a_2Cl(AA\text{-}N)]^+ + H_2O$	−2.2	−1.7			−6.0	−3.4
	$[Pt-a_2Cl(AA\text{-}O)]^+ + H_2O$	2.9	1.2			1.1	2.1
$[Pt-a_2(OH)(H_2O)]^+ + AA$	$[Pt-a_2(OH)(AA\text{-}S)]^+ + H_2O$	−14.0	−3.9			−16.1	2.7
	$[Pt-a_2(OH)(AA\text{-}N)]^+ + H_2O$	−3.1	−2.3			−7.2	−4.2
	$[Pt-a_2(OH)(AA\text{-}O)]^+ + H_2O$	2.8	1.1			3.4	5.5
$[Pt-a_2Cl(AA\text{-}S)]^+$	$[Pt-a_2(AA\text{-}S,O)]^{2+} + Cl^-$	4.2	−7.7	−4.7	−4.9	9.1	8.7
	$[Pt-a_2(AA\text{-}S,N)]^{2+} + Cl^-$	−5.3	−10.0	−14.2	−7.2	5.1	0.9
$[Pt-a_2(OH)(AA\text{-}S)]^+$	$[Pt-a_2(AA\text{-}S,O)]^+ + H_2O$	−13.4	−0.8	−27.4	−4.7	−4.3	5.9
	$[Pt-a_2(AA\text{-}S,N)]^+ + H_2O$	−22.5	−16.8	−36.5	−20.7	−15.8	−6.1
$[Pt-a_2Cl(AA\text{-}N)]^+$	$[Pt-a_2(AA\text{-}N,O)]^{2+} + Cl^-$	−1.8	1.1	−4.0	−0.6	4.2	4.8
	$[Pt-a_2(AA\text{-}S,N)]^{2+} + Cl^-$	−11.9	−5.6	−14.2	−7.2	−1.5	5.3
$[Pt-a_2(OH)(AA\text{-}N)]^+$	$[Pt-a_2(AA\text{-}N,O)]^+ + H_2O$	−21.7	−18.5	−24.8	−20.8	−14.1	−11.5
	$[Pt-a_2(AA\text{-}S,N)]^+ + H_2O$	−33.4	−18.4	−36.5	−20.7	−26.6	−7.6
$[Pt-a_2Cl(AA\text{-}O)]^+$	$[Pt-a_2(AA\text{-}S,O)]^{2+} + Cl^-$	−7.6	−6.1	−4.7	−4.9	−2.6	10.3
	$[Pt-a_2(AA\text{-}N,O)]^{2+} + Cl^-$	−6.9	−1.8	−4.0	−0.6	−0.9	1.9
$[Pt-a_2(OH)(AA\text{-}O)]^+$	$[Pt-a_2(AA\text{-}S,O)]^+ + H_2O$	−30.2	−5.8	−27.4	−4.7	−21.1	0.9
	$[Pt-a_2(AA\text{-}N,O)]^+ + H_2O$	−27.7	−21.9	−24.8	−20.8	−20.0	−15.1

[a] In all chemical formulas, a_2 means $(NH_3)_2$.

free energies of the hydroxide and chloride ions. Solvation free energies (neglecting geometry relaxation and shift in vibrational frequencies) of hydroxide ion are −106.2 kcal/mol in the DPCM/UAKS approach and −87.1 kcal/mol in the COSMO model; for chloride anion DPCM/UAKS the solvation free energy is −75.6 kcal/mol and the COSMO solvation free energy is −68.7 kcal/mol. The difference between the Cl^- and OH^- solvation free energies in the DPCM/UAKS model is therefore 30.6 kcal/mol, which almost perfectly fits the (average) experimental value of 30.3 kcal/mol.[84] However, in the COSMO model this value is about 12 kcal/mol lower.

The question whether the model of isolated molecules or the supermolecular model is more suitable for the discussion of reaction thermodynamics in aqueous environment is addressed in the next section on association and bonding energies. As will be shown later the association Gibbs free energies of all supermolecular complexes at 298.15 K are positive and thus a bigger fraction of reactants and products will not form an H-bonded complex but rather stay separated (solvated). Therefore, the results of the model of isolated molecules are more appropriate, and we refer mainly to them in the discussion.

When compared with the gas-phase results, the Gibbs free energies of the first reaction step are often very significantly reduced in absolute values. As in the gas phase, coordination of cysteine sulfur is the most exergonic for both chloro− and hydroxo−Pt complexes. Formation of the Pt−N(Cys) bond is by 6−10 kcal/mol less exergonic. The difference is higher in the case of hydroxo complexes. In the case of methionine, the Pt−S coordination is preferred only in the reaction with the hydroxo complex. With the chloro complex, the formation of the Pt−N bond is connected with a higher energy release and Pt−S coordination is even very slightly endergonical. The platinum preference for nitrogen over thioether sulfur in certain conditions was also observed in an experimental study.[85] Again the sulfur donor atom prefers the hydroxo to chloro complex more than amino group nitrogen.

The chelate-forming dissociation reactions are mostly exergonic and are usually facilitated by the presence of the solvent. This fact is the most significant in the case of reactions leading to κ^2(N,O) chelates, whose ΔG are by approximately 10 kcal/mol lower than in the gas phase. In our model, in the case of chloro complexes a +2 charged platinum chelate is formed releasing a Cl^- anion. In the case of hydroxo complexes the acidity of the +2 charged chelates is higher than that of water so that formation of a deprotonated Pt(II) +1 charged complex plus water molecule is thermodynamically preferred. The most stable structure is, similarly to the gas-phase results, the κ^2(S,N) chelate. However, in the case of the methionine, the κ^2(N,O) chelate has practically the same stability (in both COSMO and modified DPCM/UAKS models). Unlike κ^2(S,N), the methionine κ^2(N,O) chelate was not experimentally observed. The reason possibly lies in a too-high activation barrier of its formation in connection with the fact that most experimental studies were conducted at a lower pH, where the amino groups are fully protonated and thus less readily available for bonding than sulfur of the thioether. Stability of the cysteine κ^2(N,O) complex is similar to methionine also enhanced by the presence of the solvent, but the stronger sulfur bond still makes formation of the κ^2(S,N) and κ^2(S,O) chelates energetically more preferable.

The complete reaction of free amino acid with the platinum complex leading to a chelate structure is strongly exergonic. For the hydroxo complexes the released Gibbs free energy amounts up to 37 kcal/mol for cysteine and 21 kcal/mol for methionine. For the chloro complexes, these values are approximately by one-half lower. Notice that the complete platinum hydration (i.e., the hydroxo−aqua complexes in our case) strongly thermodynamically enhances formation of the chelate structures.

Bonding Energies and Association Energy Analysis. The bonding energies and association energies were calculated according to eq 3 only in the COSMO approach, and they are presented in Table 4. The DPCM/UAKS method adapted for transition metal complexes was not used mainly due to its present-time complexity, since the cavity radii modifications had to be done manually. Therefore slightly lower accuracy can be expected in comparison to reaction Gibbs free energies; nevertheless general trends should be preserved as shown later in this section. Solvation of the given system (molecule or supermolecule) and components arising from it after dissociation brings some new aspects into interpretation of the results. First, electrostatic work necessary to bring the charged (or polarized) components apart is greatly reduced, and second, in the BEs

TABLE 4: Bonding Energies (BE; kcal/mol) Calculated in the COSMO Approach

	BE	
complex[a]	Cys	Met
$[Pt-a_2Cl(AA\text{-}S)]^+$	−64.2	−50.5
$[Pt-a_2(OH)(AA\text{-}S)]^+$	−80.8	−51.6
$[Pt-a_2Cl(AA\text{-}N)]^+$	−50.1	−50.6
$[Pt-a_2(OH)(AA\text{-}N)]^+$	−73.8	−76.0
$[Pt-a_2Cl(AA\text{-}O)]^+$	−42.7	−43.3
$[Pt-a_2(OH)(AA\text{-}O)]^+$	−43.1	−43.8
$[Pt-a_2(AA\text{-}N,O)]^+$	−122.8	−123.8
$[Pt-a_2(AA\text{-}S,O)]^+$	−134.6	−115.4
$[Pt-a_2(AA\text{-}S,N)]^+$	−144.0	−127.5
$[Pt-a_2(AA\text{-}N,O)]^{2+}$	−97.2	
$[Pt-a_2(AA\text{-}S,O)]^{2+}$	−115.2	−107.3
$[Pt-a_2(AA\text{-}S,N)]^{2+}$		−119.6

[a] In all chemical formulas, a_2 means $(NH_3)_2$.

TABLE 5: Bonding Energies (kcal/mol) of the Ammine Ligands in the COSMO Approach[a]

	BE(Pt-NH_3^t)		BE(Pt-NH_3^c)	
complex[b]	Cys	Met	Cys	Met
cis-$[Pt-a_2Cl(H_2O)]^+$	−66.0	−66.0	−53.2	−53.2
cis-$[Pt-a_2(OH)(H_2O)]^+$	−62.0	−62.0	−49.2	−49.2
cis-$[Pt-a_2Cl(AA\text{-}S)]^+$	−37.5	−58.6	−48.9	−53.9
cis-$[Pt-a_2(OH)(AA\text{-}S)]^+$	−47.4	−45.4	−57.2	−51.4
cis-$[Pt-a_2Cl(AA\text{-}N)]^+$	−54.6	−53.7	−53.0	−53.1
cis-$[Pt-a_2(OH)(AA\text{-}N)]^+$	−55.4	−54.9	−63.7	−62.5
cis-$[Pt\text{-}a_2Cl(AA\text{-}O)]^+$	−56.8	−56.7	−51.9	−52.1
cis-$[Pt-a_2(OH)(AA\text{-}O)]^+$	−54.6	−54.1	−44.6	−54.1
cis-$[Pt-a_2(AA\text{-}N,O)]^+$	−54.2	−53.4	−55.8	−54.8
cis-$[Pt-a_2(AA\text{-}S,O)]^+$	−36.0	−45.9	−55.4	−54.8
cis-$[Pt-a_2(AA\text{-}S,N)]^+$	−37.1	−50.0	−52.8	−52.5
cis-$[Pt-a_2(AA\text{-}N,O)]^{2+}$	−59.5		−66.2	
cis-$[Pt-a_2(AA\text{-}S,O)]^{2+}$	−39.0	−48.0	−63.3	−58.4
cis-$[Pt-a_2(AA\text{-}S,N)]^{2+}$		−49.8		−55.0

[a] NH_3^t is the ammine ligand trans to aqua ligand in the reactant complexes, the amino acid donor atom in the monodentate complexes, the sulfur donor atom in κ^2(S,N) and κ^2(S,O) chelates, and the amino group nitrogen in the κ^2(N,O) complexes. NH_3^c is the second ammine ligand. [b] In all chemical formulas, a_2 means $(NH_3)_2$.

calculation, direct solvation of atoms which participated in broken bond can be an unwanted effect, which actually never occurs.

All the BEs are generally smaller in their absolute value when compared with the gas-phase counterparts. Lowering of the absolute BE values during transition from the gas phase to solvent occurs systematically to a higher extent in the chloro complexes (by approximately 10 kcal/mol). This effect is mainly caused by an energetically more advantageous solvation of the chloride-containing fragment in comparison to the entire complex (due to a larger accessible surface of chloride in the fragment). Generally, BEs of solvated chelates are reduced to roughly one-third of gas-phase values since the electrostatic work required for the separation of charged parts is substantially diminished (proportionally to $1/\varepsilon_r$). The only exceptions to this rule are Pt−N bonds in monodentate hydroxo complexes, which will be discussed later.

Comparing the BE of the weakest Pt−O bond, a similar bonding energy of about 43 kcal/mol is obtained for all forms of monodentate Pt complexes with both amino acids in hydroxo and chloro structures (cf. Table 4). In the case of the nitrogen adducts, the BE(Pt−N) values are similar for both amino acids—approximately 75 kcal/mol in the hydroxo complexes and approximately 50 kcal/mol in the chloro complexes. The Pt−S bonds demonstrate the highest variation. They are the strongest in the cysteine adducts. In the methionine hydroxo complex the BE(Pt−S) is weaker than the corresponding Pt−N energy. In the semihydrated (chloro) complex, both (BE(Pt−N) and BE(Pt−S)) energies are comparable. The trend for the BE energies of the Pt−X bond in the hydroxo complexes does not correlate completely with the trend of reaction energies. The higher BEs (in absolute values) of Pt−N bonds result from the proton transfer from amino acid to hydroxo ligand of the Pt complex. This proton transfer causes (a) a stronger electrostatic interaction between the −1 charged amino acid and +2 platinum moiety, which is only partially compensated by higher solvation energies of both parts (AA^- and Pt^{2+}), and (b) a lower competitive donation ability of the (neutral) aqua ligand to the Pt atom in comparison with the negatively charged OH^- group. In this way a stronger Pt−N(AA) interaction is obtained. In the chelate complexes, the BEs could be quite successfully used to predict their relative thermodynamic preferences. Nevertheless, in the case of κ^2(N,O) complexes, the relatively low BEs seems to slightly underestimate the resulting thermodynamic stability of the complexes. In the case of +2 charged complexes there is a quite large difference between the relative BEs and relative reaction Gibbs free energies, but the qualitative trend is still preserved.

BEs of platinum−ammine ligand bonds are collected in Table 5. The largest trans influence leading to the weakening of the Pt−NH_3^t bond by up to 30 kcal/mol is induced by S(Cys) in monodentate chloro and chelate complexes. In hydroxo complexes, the trans influence of cysteine sulfur is comparable to methionine—it causes a reduction of the BE(Pt−NH_3^t) by ca. 15 kcal/mol in comparison with the reactant complex. A remarkably smaller trans influence of the methionine S-donor atom can be seen in the Pt−chloro−methionine complex, where even nitrogen of the amino group and oxygen of the carboxyl group exhibit larger weakening of the Pt−NH_3^t bond. This is in very good accord with the above-mentioned thermodynamics of methionine monodentate coordination. Trans influence of the carboxyl group oxygen and nitrogen from amino group of methionine is generally similar and causes a weakening of the Pt−NH_3^t bond by about 10 kcal/mol. No significant change of trans influence of individual groups was observed upon the chelation step, except for the fact that protonation to the +2 species generally leads to a strengthening of Pt−NH_3 bonds.

The association energies of H-bonded parts of supermolecule calculated from eq 4 are reduced more than twice in comparison to the gas-phase values. As follows from Table 6, the highest association energies are in the reactant supermolecules of the first reaction step: *cis*-$[Pt(NH_3)_2Cl(H_2O)]^+$ and *cis*-$[Pt(NH_3)_2(OH)(H_2O)]^+$, where two H-bonds are present between the carboxylic group oxygens and hydrogens of aqua and ammine Pt ligands (cf. Figure 2). This coordination differs from the reactant arrangement in the gas phase where carboxyl oxygen forms an H-bond with the NH_3 ligand and the amino group forms an H-bond with the aqua ligand. Protonation of the amino group in solvent prevents such an H-bonding pattern. The association energies of monodentate complexes and water molecule released in the first reaction step are approximately 3−6 kcal/mol. The lowest values are seen in supermolecules composed of water and κ(O) complexes where the "best sites" to create an H-bond (the carboxyl group or aqua ligand) are not available. A similar situation occurs in the supermolecules representing products of the second reaction step of the hydroxo com-

TABLE 6: Association Energies (kcal/mol) at 298.15 K, in the COSMO Approach

complex[a]	ΔE_S[a] Cys	ΔE_S[a] Met	ΔG_S[a] Cys	ΔG_S[a] Met
cis-[Pt−a_2Cl(H_2O)]$^+$ + AA	−12.0	−12.5	1.9	1.5
cis-[Pt−a_2(OH)(H_2O)]$^+$ + AA	−10.7	−11.4	3.2	2.7
cis-[Pt−a_2Cl(AA-S)]$^+$ + H_2O	−5.3	−8.2	4.1	6.5
cis-[Pt−a_2(OH)(AA-S)]$^+$ + H_2O	−4.4	−8.2	6.4	7.8
cis-[Pt−a_2Cl(AA-N)]$^+$ + H_2O	−5.2	−4.8	3.9	4.5
cis-[Pt−a_2(OH)(AA-N)]$^+$ + H_2O	−4.4	−5.1	6.4	4.8
cis-[Pt−a_2Cl(AA-O)]$^+$ + H_2O	−3.6	−3.2	7.3	7.4
cis-[Pt−a_2(OH)(AA-O)]$^+$ + H_2O	−2.4	−1.5	9.9	12.8
cis-[Pt−a_2(AA-N,O)]$^{2+}$ + Cl^-	−10.2	−9.9	−7.1	−7.5
cis-[Pt−a_2(AA-N,O)]$^+$ + H_2O	−3.4	−3.1	7.0	7.5
cis-[Pt−a_2(AA-S,O)]$^{2+}$ + Cl^-	−10.0	−6.0	−6.1	4.0
cis-[Pt−a_2(AA-S,O)]$^+$ + H_2O	−3.1	−4.0	7.6	6.5
cis-[Pt−a_2(AA-S,N)]$^{2+}$ + Cl^-	−7.0	−7.4	−0.6	1.6
cis-[Pt−a_2(AA-S,N)]$^+$ + H_2O	−5.0	−3.2	4.2	10.2

[a] In all chemical formulas, a_2 means $(NH_3)_2$.

TABLE 7: Association Free Energies (kcal/mol) of the Second Reaction Step Products at 298.15 K Calculated in the COSMO and DPCM/UAKS Approach without BSSE Corrections

complex[a]	ΔG_S[a] (COSMO) Cys	ΔG_S[a] (COSMO) Met	ΔG_S[a] (DPCM) Cys	ΔG_S[a] (DPCM) Met
cis-[Pt−a_2(AA-N,O)]$^{2+}$ + Cl^-	−7.7	−8.1	4.9	3.7
cis-[Pt−a_2(AA-N,O)]$^+$+ H_2O	6.4	7.0	6.8	6.9
cis-[Pt−a_2(AA-S,O)]$^{2+}$ + Cl^-	−6.9	3.1	6.0	16.4
cis-[Pt−a_2(AA-S,O)]$^+$+ H_2O	7.2	6.0	9.1	6.7
cis-[Pt−a_2(AA-S,N)]$^{2+}$ + Cl^-	−1.2	1.0	10.4	10.9
cis-[Pt−a_2(AA-S,N)]$^+$+ H_2O	3.9	9.7	7.6	10.7

[a] In all chemical formulas, a_2 means $(NH_3)_2$.

plexes, where association energies of the water molecule are comparatively low. The exceptions are the *cis*-[Pt$(NH_3)_2$(Cys-S,N)]$^+$ + H_2O and *cis*-[Pt$(NH_3)_2$(Met-S,O)]$^+$ + H_2O supermolecules, where the carboxyl group is available to participate in the H-bonding. The chloride anion associations are stronger with energies around −10 kcal/mol.

When contributions of nuclear motion are taken into account, we obtain the true association Gibbs free energies (ΔG_S[a]). They are collected in the last two columns of Table 7. From these values it follows that the ΔG_S[a] association energies are positive in all cases except of the supermolecules representing products of the second reaction step, where the chloride anion is released and H-bonded to the metallocomplex. Association energy analysis was not performed in DPCM/UAKS approach, but it is possible to obtain BSSE uncorrected association energies of final product supermolecules from the difference between the reaction energies of the second reaction step in the model of isolated molecules and the supermolecular approach. Contrary to the COSMO results, positive association ΔG_S[a] were obtained also for supermolecules containing chloride ion. This difference basically lies in a significantly lower COSMO chlorine ion solvation free energy as discussed above. The comparison of BSSE uncorrected COSMO and DPCM/UAKS association Gibbs free energies is summarized in Table 8 of the Supporting Information. In the case of supermolecules representing the final products of reactions of hydroxo complexes (consisting of a +1 e charged chelate and a water molecule) both methods match fairly well. But for the +2 charged complexes with a chloride anion, the DPCM/UAKS values are higher by slightly more than 10 kcal/mol. Therefore, we can conclude that when no small anion such as chloride or hydroxide is present, the COSMO values are relatively reliable and similar to results obtained using the modified DPCM/UAKS model. Correcting the value obtained for the chloride ion containing supermolecules, all association Gibbs free energies of all molecules are thus positive. On the basis of this fact, we propose that the model of isolated (solvated) molecules is more appropriate for description of reaction thermodynamics in this case.

Conclusions

In the present study we explored cisplatin interactions with sulfur-containing amino acids in the polarizable continuum model. Optimizations of semihydrated and fully hydrated cisplatin complex with cysteine and methionine were performed at the B3LYP/6-31+G(d)/COSMO level of calculations. We suggested a two-step reaction mechanism: the first substitution step where the aqua ligand was replaced by one of the three active amino acid sites (N, O, or S), and the second dissociation process forming chelate and water or chloride anion. All the reactants and products were treated as supermolecular complexes as well as an approximation of isolated molecules. Energy characteristics and electronic properties were determined at the B3LYP/6-311++G(2df,2pd) level using two different PCM models—the COSMO and DPCM techniques with different cavities. Obtained results were compared with the gas-phase data from our previous study where a similar computational model was used.

The first reaction step is exergonic for both amino acids and both platinum complexes. The reaction Gibbs free energies released in formation of the Pt−N adduct are roughly comparable for both amino acids; the same also holds for the Pt−O adducts. However, in the case of Pt−S coordination, the energy of the cysteine-complex formation is more exergonic than for methionine (by 7−10 kcal/mol). Generally, cysteine strongly prefers the κ(S) coordination over κ(N). Creation of the κ(O) complex is thermodynamically the least convenient reaction outcome. Thermodynamics of reaction with methionine is dependent on the cisplatin hydration state. In the case of the monohydrated chloro complex, the κ(N) coordination is the most exergonic. On the other hand, the κ(S(Met)) bonding is more preferable in the hydroxo complex. A similar (but less pronounced) behavior was observed also in the gas phase.

Among products of the chelation process the κ^2(S,N) chelate of cysteine clearly prevails followed by almost an equivalent presence of the κ^2(S,O) and κ^2(N,O) structures. This is in qualitative agreement with gas-phase calculations. In the methionine case, the highest ΔG release occurs in the formation of the κ^2(N,O) and κ^2(S,N) chelates. The κ^2(S,O) structure is predicted to be the least stable using both SCRF methods. This preference however differs from the gas-phase results, where κ^2(S,O) and κ^2(S,N) complexes are more stable than the κ^2(N,O) complex.

Two procedures for calculation of BSSE-corrected bonding and association energies were explored. The first calculates the BSSE correction directly with ghost functions placed outside of a solute cavity, whereas the second calculates the correction separately in the cavity of the original supermolecule. Analysis of Gibbs free association energies showed that the model of isolated molecules is more suitable for discussion of thermodynamics of considered reactions in aqueous solution than the supermolecular model due to the positive Gibbs free association energies of all supermolecules. Basic thermodynamic preferences of considered reactions are relatively well-reflected in bonding energies of Pt−AA bonds. Some care must be, however, taken due to the effects of intermolecular proton transfers and solvation of residues.

Acknowledgment. This study was supported by the MSM 0021620835 grant of the Ministry of Education, Youth and Sport and the IAA400550701 grant of the Grant Agency of the Academy of Sciences of the Czech Republic. We are grateful for access to the excellent computational resources from our department supercomputer cluster administered by Dr. Šimánek.

Supporting Information Available: Table showing reaction Gibbs free energies using the COSMO approach. This material is available free of charge via the Internet at http://pubs.acs.org.

References and Notes

(1) Eastman, A. The Mechanism of Action of Cisplatin: From Adducts to Apoptosis. In *Cisplatin*; Lippert, B., Ed.; Wiley-VCH: Weinheim, Germany, 1999; p 111.
(2) Pascoe, J. M.; Roberts, J. J. *Biochem. Pharmacol.* **1974**, *23*, 1345.
(3) Lippert, B. *Cisplatin: Chem. and Biochemistry of a Leading Anticancer Drug.*; Wiley-VCH: Wienheim, Germany, 1999; p 1999.
(4) Donahue, B. A.; Augot, M.; Bellon, S. F.; Treiber, D. K.; Toney, J. H.; Lippard, S. J.; Essigmann, J. M. *Biochemistry* **1990**, *29*, 5872.
(5) Peleg-Shulman, T.; Najajreh, Y.; Gibson, D. *J Inorg. Biochem.* **2002**, *91*, 306.
(6) Kartalou, M.; Essigmann, J. M. *Mutat. Res.* **2001**, *478*, 1.
(7) Fojta, M.; Pivonkova, H.; Brazdova, M.; Kovarova, L.; Palecek, E.; Pospisilova, S.; Vojtesek, B.; Kasparkova, J.; Brabec, V. *Biochem. Pharmacol.* **2003**, *65*, 1305.
(8) Pivonkova, H.; Pecinka, P.; Ceskova, P.; Fojta, M. *FEBS J* **2006**, *273*, 4693.
(9) Andrews, P. A.; Jones, J. A. *Cancer Commun.* **1991**, *3*, 1.
(10) Burger, A. M.; Double, J. A.; Newell, D. R. *Eur. J. Cancer* **1997**, *33*, 638.
(11) Zamble, D. B.; Lippard, S. J. The Responce of Cellular Proteins to Cisplatin-Damaged DNA. In *Cisplatin*; Lippert, B., Ed.; Wiley-VCH: Weinheim, Germany, 1999; p 73.
(12) Meister, A. *J. Biol. Chem.* **1988**, *263*, 17205.
(13) Schafer, F. Q.; Buettner, G. R. *Free Radical Biol. Med.* **2001**, *30*, 1191.
(14) Ishikawa, T.; Aliosman, F. *J. Biol. Chem.* **1993**, *268*, 20116.
(15) Appleton, T. G.; Connor, J. W.; Hall, J. R.; Prenzler, P. D. *Inorg. Chem.* **1989**, *28*, 2030.
(16) Witte, A. B.; Anestal, K.; Jerremalm, E.; Ehrsson, H.; Arner, E. S. J. *Free Radical Biol. Med.* **2005**, *39*, 696.
(17) Arner, E. S. J.; Nakamura, H.; Sasada, T.; Yodoi, J.; Holmgren, A.; Spyrou, G. *Free Radical Biol. Med.* **2001**, *31*, 1170.
(18) Townsend, D. M.; Deng, M.; Zhang, L.; Lapus, M. G.; Hanigan, M. H. *J Am. Soc. Nephrol.* **2003**, *14*, 1.
(19) Zhang, L.; Hanigan, M. H. *Pharmacol. Exp. Ther.* **2003**, *306*, 988.
(20) Rudin, C. M.; Yang, Z.; Schumaker, L. M.; VanderWeele, D. J.; Newkirk, K.; Egorin, M. J.; Zuhowski, E. G.; Cullen, K. J. *Cancer Res.* **2003**, *63*, 312.
(21) Nagata, J.; Kijima, H.; Hatanaka, H.; Asai, S.; Miyachi, H.; Takagi, A.; Miwa, T.; Mine, T.; Yamazaki, H.; Nakamura, M.; Kondo, T.; Scanlon, K. J.; Ueyama, Y. *Biochem. Biophys. Res. Commun.* **2001**, *286*, 406.
(22) Reedijk, J.; Teuben, J. M. Platinum-Sulphur Interaction Involved in Antitumor Drugs, Rescue Agents and Biomolecules. In *Cisplatin*; Lippert, B., Ed.; Wiley-VCH: Weinheim, Germany, 1999.
(23) Norman, R. E.; Ranford, J. D.; Sadler, P. J. *Inorg. Chem.* **1992**, *31*, 877.
(24) Williams, K. M.; Rowan, C.; Mitchell, J. *Inorg. Chem.* **2004**, *43*, 1190.
(25) Appleton, T. G.; Connor, J. W.; Hall, J. R. *Inorg. Chem.* **1988**, *27*, 130.
(26) Wei, H. Y.; Liu, Q.; Lin, J.; Jiang, P. J.; Guo, Z. J. *Inorg. Chem. Commun.* **2004**, *7*, 792.
(27) Riley, C. M.; Sternson, L. A.; Repta, A. J. *J. Pharm. Sci.* **1983**, *72*, 351.
(28) Reedijk, J. *Chem. Rev.* **1999**, *99*, 2499.
(29) Vrana, O.; Brabec, V. *Biochemistry* **2002**, *41*, 10994.
(30) Manka, S.; Becker, F.; Hohage, O.; Sheldrick, W. S. *J Inorg. Biochem.* **2004**, *98*, 1947.
(31) Hohage, O.; Sheldrick, W. S. *J Inorg. Biochem.* **2006**, *100*, 1506.
(32) Bose, R. N.; Ghosh, S. K.; Moghaddas, S. *J Inorg. Biochem.* **1997**, *65*, 199.
(33) Lau, J. K. C.; Deubel, D. V. *Chem.−Eur. J* **2005**, *11*, 2849.
(34) Zimmermann, T.; Zeizinger, M.; Burda, J. V. *J. Inorg. Biochem.* **2005**, *99*, 2184.
(35) Hagrman, D.; Goodisman, J.; Souid, A.-K. J. *Pharm. Exp. Ther.* **2004**, *308*, 658.
(36) Dabrowiak, J. C.; Goodisman, J.; Souid, A.-K. *Drug Metab. Dispos.* **2002**, *30*, 1378.
(37) Dedon, P. C.; Borch, R. F. *Biochem. Pharmacol.* **1987**, *36*, 1955.
(38) Bose, R. N.; Moghaddas, S.; Weaver, E. L.; Cox, E. H. *Inorg. Chem.* **1995**, *34*, 5878.
(39) Zou, J.; Yang, X. D.; An, F.; Wang, K. *J. Inorg. Biochem.* **1998**, *70*, 227.
(40) Da Silva, V. J.; Costa, L. A. S.; Dos Santos, H. F. *Int. J. Quantum Chem.* **2008**, *108*, 401.
(41) Matsui, T.; Shigeta, Y.; Hirao, K. *Chem. Phys. Lett.* **2006**, *423*, 331.
(42) Dal Peraro, M.; Ruggerone, P.; Raugei, S.; Gervasi, F. L.; Carloni, P. *Curr. Opin. Struct. Biol.* **2007**, *17*, 149.
(43) Chang, G. R.; Zhou, L. X.; Chen, D. *Chin. J. Struct. Chem.* **2006**, *25*, 533.
(44) Dos Santos, H. F.; Marcial, B. L.; De Miranda, C. F.; Costa, L. A. S.; De Almeida, W. B. *J. Inorg. Biochem.* **2006**, *100*, 1594.
(45) Lopes, J. F.; Menezes, V. S. D.; Duarte, H. A.; Rocha, W. R.; De Almeida, W. B.; Dos Santos, H. F. *J. Phys. Chem. B* **2006**, *110*, 12047.
(46) Costa, L. A.; Hambley, T. W.; Rocha, W. R.; Almeida, W. B.; Dos Santos, H. F. *Int. J. Quantum Chem.* **2006**, *106*, 2129.
(47) Robertazzi, A.; Platts, J. A. *J. Comput. Chem.* **2004**, *25*, 1060.
(48) Robertazzi, A.; Platts, J. A. *Inorg. Chem.* **2005**, *44*, 267.
(49) Robertazzi, A.; Platts, J. A. *Chem.−Eur. J* **2006**, *12*, 5747.
(50) Wysokinski, R.; Hernik, K.; Szostak, R.; Michalska, D. *Chem. Phys.* **2007**, *333*, 37.
(51) Yuan, Q. H.; Zhou, L. X. *Chin. J. Struct. Chem.* **2007**, *26*, 962.
(52) Erturk, H.; Hofmann, A.; Puchta, R.; van Eldik, R. *Dalton Trans.* **2007**, 2295.
(53) Hao, L.; Zhang, Y.; Tan, H. W.; Chen, G. J. *Chem. J. Chin. Univ. (Chinese)* **2007**, *28*, 1160.
(54) Pavelka, M.; Lucas, M. F. A.; Russo, N. *Chem. Eur. J.*, in press.
(55) Hofmann, A.; Jaganyi, D.; Munro, O. Q.; Liehr, G.; van Eldik, R. *Inorg. Chem.* **2003**, *42*, 1688.
(56) Cooper, J.; Ziegler, T. *Inorg. Chem.* **2002**, *41*, 6614.
(57) Zhu, H. J.; Ziegler, T. J. *Organomet. Chem.* **2006**, *691*, 4486.
(58) Tsipis, A. C.; Sigalas, M. P. *J. Mol. Struct.* **2002**, *584*, 235.
(59) Zhu, C.; Raber, J., A., E. L. *J. Phys. Chem. B* **2005**, *109*, 12195.
(60) Song, T.; Hu, P. *J. Chem. Phys.* **2006**, *125*, 091101.
(61) Jia, M.; Qu, W.; Yang, Z.; Chen, G. *Int. J. Mod. Phys. B* **2005**, *19*, 2939.
(62) Zhang, Y.; Guo, Z.; You, X.-Z. *J. Am. Chem. Soc.* **2001**, *123*, 9378.
(63) Lau, J. K. C.; Deubel, D. V. *J Chem. Theor. Comput.* **2006**, *2*, 103.
(64) Parr, R. G.; Pearson, R. G. *J. Am. Chem. Soc.* **1983**, *105*, 7512.
(65) Hush, N. S.; Schamberger, J.; Bacskay, G. B. *Coord. Chem. Rev.* **2005**, *249*, 299.
(66) Wysokinski, R.; Michalska, D. J. *Comput. Chem.* **2001**, *22*, 901.
(67) Andrae, D.; Haussermann, U.; Dolg, M.; Stoll, H.; Preuss, H. *Theor. Chim. Acta* **1990**, *77*, 123.
(68) Bergner, A.; Dolg, M.; Kuchle, W.; Stoll, H.; Preuss, H. *Mol. Phys.* **1993**, *80*, 1431.
(69) Burda, J. V.; Zeizinger, M.; Sponer, J.; Leszczynski, J. *J. Chem. Phys.* **2000**, *113*, 2224.
(70) Klamt, A.; Schuurmann, G. *J Chem. Soc., Perkin Trans.* **2 1993**, 799.
(71) Miertus, S.; Scrocco, E.; Tomasi, *J. Chem. Phys.* **1981**, *55*, 117.
(72) Miertus, S.; Tomasi, *J. Chem. Phys.* **1982**, *65*, 239.
(73) Barone, V.; Cossi, M.; Tomasi, J. *J. Chem. Phys.* **1997**, *107*, 3210.
(74) Zimmermann, T.; Burda, J. V. *PCCP*, submitted for publication.
(75) da Silva, G.; Kennedy, E. M.; Dlugogorski, B. Z. *J. Phys. Chem. A* **2006**, *110*, 11371.
(76) Boys, S. F.; Bernardi, F. *Mol. Phys.* **1970**, *19*, 553.
(77) van Duijneveldt, F. B.; van Duijneveldt-van de Rijdt, J. G. C. M.; van Lenthe, J. H. *Chem. Rev.* **1994**, *94*, 1873.
(78) Weinhold, F. *NBO 5.0 Program*, 5.0 ed.; University of Wisconsin: Madison, WI, 2001.
(79) Heudi, O.; Cailleux, A.; Allain, P. *J Inorg. Biochem.* **1998**, *71*, 61.
(80) Fernandez-Ramos, A.; Cabaleiro-Lago, E.; Hermida-Ramon, J. M.; Martinez-Nunez, E.; Pena-Gallego, A. *J. Mol. Struct.* **2000**, *498*, 191.
(81) Deubel, D. V. *J. Am. Chem. Soc.* **2002**, *124*, 5834.
(82) Fuks, L.; Sadlej-Sosnowska, N.; Samochocka, K.; Starosta, W. *J. Mol. Struct.* **2005**, *740*, 229.
(83) Wilson, C.; Scudder, M. L.; Hambley, T. W.; Freeman, H. C. *Acta Cryst., Sect. C: Cryst. Struct. Commun.* **1992**, *48*, 1012.
(84) Tissandier, M. D.; Cowen, K. A.; Feng, W. Y.; Gundlach, E.; Cohen, M. H.; Earhart, A. D.; Coe, J. V.; Tuttle, T. R. *J. Phys. Chem. A* **1998**, *102*, 7787.
(85) Lempers, E. L. M.; Reedijk, J. J. *Inorg. Chem.* **1990**, *29*, 1880.

JP807645X